# Fractional Quantum Hall States at $\nu = 13/5$ and $12/5$ and Their Non-Abelian Nature

W. Zhu,[1,2] S. S. Gong,[2] F. D. M. Haldane,[1] and D. N. Sheng[2]
[1]Department of Physics, Princeton University, Princeton, New Jersey 08544, USA
[2]Department of Physics and Astronomy, California State University, Northridge, California 91330, USA
(Received 25 May 2015; revised manuscript received 9 July 2015; published 18 September 2015)

Topological quantum states with non-Abelian Fibonacci anyonic excitations are widely sought after for the exotic fundamental physics they would exhibit, and for universal quantum computing applications. The fractional quantum Hall (FQH) state at a filling factor of $\nu = 12/5$ is a promising candidate; however, its precise nature is still under debate and no consensus has been achieved so far. Here, we investigate the nature of the FQH $\nu = 13/5$ state and its particle-hole conjugate state at $12/5$ with the Coulomb interaction, and we address the issue of possible competing states. Based on a large-scale density-matrix renormalization group calculation in spherical geometry, we present evidence that the essential physics of the Coulomb ground state (GS) at $\nu = 13/5$ and $12/5$ is captured by the $k = 3$ parafermion Read-Rezayi state ($RR_3$), including a robust excitation gap and the topological fingerprint from the entanglement spectrum and topological entanglement entropy. Furthermore, by considering the infinite-cylinder geometry (topologically equivalent to torus geometry), we expose the non-Abelian GS sector corresponding to a Fibonacci anyonic quasiparticle, which serves as a signature of the $RR_3$ state at $13/5$ and $12/5$ filling numbers.

DOI: 10.1103/PhysRevLett.115.126805 PACS numbers: 73.43.-f, 03.67.Mn, 05.30.Pr

*Introduction.*—While fundamental particles in nature are either bosons or fermions, the emergent excitations in two-dimensional strongly correlated systems may obey fractional or anyonic statistics [1,2]. After two decades of study [3–13], current interest in exotic excitations focuses on states of matter with non-Abelian quasiparticle excitations [14–16], and their potential applications to the rapidly evolving field of quantum computation and cryptography [17–22]. So far, the most promising platform for realization of non-Abelian statistics is the fractional quantum Hall (FQH) effect in the first excited Landau level, and two of the most interesting examples are at the filling factors of $\nu = 5/2$ and $12/5$. The $\nu = 5/2$ state is widely considered to be a candidate for the Moore-Read state hosting non-Abelian Majorana quasiparticles [14–16]. Experiments have revealed that the $12/5$ state appears to behave differently from the conventional FQH effect [5,8], and it may also be a candidate state for hosting non-Abelian excitations. However, the exact nature of the FQH $12/5$ state is still undetermined due to the existence of other possible competing candidate states.

Several ground-state (GS) wave functions have been proposed [16,23–27] as models for the observed FQH effect at $\nu = 12/5$ [5,8,13]. The most exciting candidate is the $k = 3$ parafermion state proposed by Read and Rezayi ($RR_3$) [16]. This $RR_3$ state describes a condensate of three-electron clusters that forms an incompressible state at $\nu = 13/5$ [16]. One can also construct the particle-hole partner of the $RR_3$ state to describe the $12/5$ FQH effect. Besides the $RR_3$ state, some competing candidates for $\nu = 13/5$ or $12/5$ exist: a hierarchy state [28,29], a Jain composite-fermion (CF) state [30], a generalization of the non-Abelian Pfaffian state by Bonderson and Slingerland (BS) [24,25], and a bipartite CF state [26,27]. So far, the true nature of the $12/5$ and $13/5$ FQH states remains undetermined. The main challenges in settling this issue are the limited computational ability and the lack of an efficient diagnostic method. For example, from exact diagonalization (ED) calculations in the limited feasible range of system sizes, it is found that the overlaps between the Coulomb GS at $\nu = 12/5$ and different model wave functions are all relatively large [16,25], while the extrapolated GS energies of the $RR_3$ and BS states are very close in the thermodynamic limit [25,31]. Taken as a whole, previous studies have left the nature of the Coulomb GS at $\nu = 13/5$ and $12/5$ unsettled.

Recently, there has been growing interest in connecting quantum entanglement [32–35] with emergent topological order [36,37] in strongly interacting systems, which offers a new route to identification of the precise topological order of a many-body state. Although characterization of entanglement has been successfully used to identify various well-known types of topological order [38–45], application of the method to a system with competing phases still faces challenges when ED studies suffer from strong finite-size effects, and other methods such as quantum Monte Carlo calculations suffer from sign problems. The recent development of the high efficiency density-matrix renormalization group (DMRG) in momentum space [42,46] allows the study of such systems in sphere and cylinder geometries, both of which can be used to make concrete predictions of the physics of real systems in the thermodynamic limit.

 

Here, we combine these advances and use these two geometries to address the long-standing issues of the FQH at $\nu = 12/5$ and $13/5$.

In this Letter, we study the FQH at the $\nu = 12/5$ and $13/5$ filling factors by using the state-of-the-art DMRG numerical simulations. By studying large systems up to $N_e = 36$ on spherical geometry, we establish that the Coulomb GS at $\nu = 13/5$ is an incompressible FQH state, protected by a robust neutral-excitation gap $\Delta_n \approx 0.012(e^2/l_B)$. Crucially, we show that the entanglement spectrum (ES) fits the corresponding $SU(2)_3$ conformal field theory (CFT) which describes the edge structure of the parafermion $RR_3$ state. The topological entanglement entropy (TEE) is also consistent with the predicted value for the $RR_3$ state, indicating the emergence of Fibonacci anyonic quasiparticles. Moreover, we also perform a finite-size scaling analysis of the GS energies for $\nu = 12/5$ states at different shifts corresponding to the particle-hole conjugate of the $RR_3$ state, the Jain state and the BS state. Finite-size scaling confirms that the ground state with topological shift $\mathcal{S} = -2(3)$ (where $RR_3$ and its particle-hole partner states are expected to occur) is energetically favored in the thermodynamic limit. Finally, to explicitly demonstrate the topological degeneracy, we obtain two topologically distinct GS sectors on the infinite cylinder using infinite-size DMRG. While one sector is the identity sector matching to the GS from the sphere, the new sector is identified as the non-Abelian sector with a Fibonacci anyonic quasiparticle through its characteristic ES and TEE. Thus, we establish that the essence of the FQH state at $\nu = 13/5$ is fully captured by the non-Abelian parafermion $RR_3$ state (and by its particle-hole conjugate at $\nu = 12/5$) and show that it is stable against perturbations as we change the Haldane pseudopotentials and the layer width of the system.

*Model and method.*—We use the Haldane representation [28,47,48] in which the $N_e$ electrons are confined on the surface of a sphere surrounding a magnetic monopole of strength $Q$. In this case, the orbitals of the $n$th Landau level are represented as orbitals with azimuthal angular momentum $-L, -L+1, \ldots, L$, with $L = Q + n$ being the total angular momentum. The total magnetic flux through the spherical surface is quantized to be an integer $N_s = 2L$. Assuming that electron spins are fully polarized and neglecting Landau-level mixing, the Hamiltonian in the spherical geometry can be written as

$$H = \frac{1}{2} \sum_{m_1+m_2=m_3+m_4} \langle m_1, m_2|V|m_3, m_4\rangle \hat{a}^\dagger_{m_1} \hat{a}^\dagger_{m_2} \hat{a}_{m_3} \hat{a}_{m_4},$$

where $\hat{a}^\dagger_m$ ($\hat{a}_m$) is the creation (annihilation) operator at the orbital $m$ and $V$ is the Coulomb interaction between electrons in units of $e^2/l_B$, with $l_B$ being the magnetic length. The two-body Coulomb interaction element can be decomposed as

$$\langle i, j|V|p, q\rangle = \sum_{l=0}^{2L} \sum_{m=-l}^{l} \langle L, i; L, j|l, m\rangle \langle l, m|L, p; L, q\rangle \mathcal{V}^n(l),$$

where $\langle L, i; L, j|l, m\rangle$ are the Clebsch-Gordan coefficients and $\mathcal{V}^n(l)$ is the Haldane pseudopotential representing the pair energy of two electrons with relative angular momentum $2L - l$ in the $n$th LL [28,49]. For electrons at fractional filling factor $\nu$, $N_s = \nu^{-1} N_e - \mathcal{S}$, where $\mathcal{S}$ is the curvature-induced "shift" on the sphere.

Our calculation is based on the unbiased DMRG method [46,56–60], combined with ED. The (angular) momentum-space DMRG allows us to use the total electron number $N_e$ and the total $z$ component of angular momentum $L_z^{\text{tot}} = \sum_{i=1}^{N_e} m_i$ as good quantum numbers to reduce the Hilbert subspace dimension [46]. Here, we report the result at $\nu = 13/5(12/5)$ with an electron number up to $N_e = 36(22)$ by keeping up to 30 000 states with optimized DMRG, which allows us to obtain accurate results for energy and the ES on much larger system sizes beyond the ED limit [$N_e^{\text{ED}} = 24(16)$ at $\nu = 13/5(12/5)$].

*Ground state energy, energy spectrum, and neutral gap.*—We first compute the GS energies for a number of systems up to $N_e = 36$ at $\nu = 13/5$, with a shift $\mathcal{S} = 3$ consistent with the $RR_3$ state. As shown in the low-lying energy spectrum in the inset of Fig. 1(b) obtained from ED for $N_e = 21$, the GS is located in the $L^{\text{tot}} = 0$ sector and is separated from the higher energy continuum by a finite gap, which signals an incompressible FQH state. The extrapolation of the GS energy to the thermodynamic limit can be carried out using a quadratic function of $1/N_e$ (the blue line), or a linear fit in $1/N_e$ (the red line) after renormalizing the energy by $\sqrt{2Q\nu/N_e}$ to take into account the curvature of the sphere [61], as shown in Fig. 1(a). We obtain the $E_0/N_e = -0.38458(24)$ (the blue line) and $-0.38487(9)$ (the red line), which demonstrates consistency between the two extrapolating schemes.

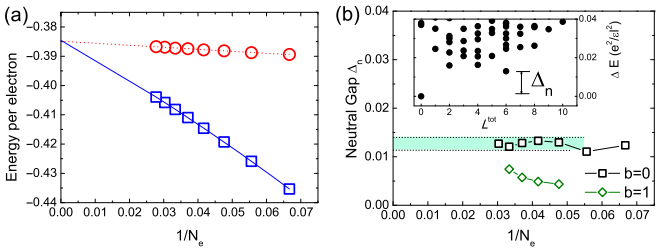


FIG. 1 (color online). (a) The ground-state energy per electron (the blue dots) corresponding to the $\nu = 13/5$ state. The blue line shows the extrapolated values obtained using a quadratic function of $1/N_e$. The red dots shows the rescaling energy by a renormalized magnetic length and the red line is the linear fitting. (b) The neutral gap $\Delta_n$ for the $13/5$ state as a function of the $1/N_e$ ($b$ is the layer-width parameter [49]). (Inset) Energy spectrum versus total angular momentum $L^{\text{tot}}$ for $N_e = 21$. $\Delta_n$ is defined as the energy difference between the lowest-energy state (in $L^{\text{tot}} = 0$) and the first excited state (in $L^{\text{tot}} \neq 0$).

We also calculated the neutral-excitation gap $\Delta_n$ at $\nu = 13/5$ [62]. This is equivalent to the energy difference between the GS and the "roton minimum" [63–65], as illustrated in the inset of Fig. 1(b). The roton minimum corresponds to the lowest excitation energy of a quasielectron-quasihole pair [65]. Figure 1(b) shows $\Delta_n$ as a function of $1/N_e$, where the large-system results indicate that the neutral gap approaches a nonzero value $\Delta_n \approx 0.012 \pm 0.001$ for $N_e \geq 21$. Since the Hamiltonian in this Letter is particle-hole symmetric, the neutral gap at $\nu = 12/5$ and $13/5$ is expected to be identical [66]. In addition, if the effect of finite layer width is considered [49], the neutral-excitation gap is reduced but still remains consistent with a nonzero value [Fig. 1(b)].

*Competing states.*—In Fig. 2, we compare the GS energies per electron of three known candidates for $\nu = 12/5$: the particle-hole conjugate of the $RR_3$ state with a shift $\mathcal{S} = -2$, the non-Abelian BS state with $\mathcal{S} = 2$ [24], and a Jain state with $\mathcal{S} = 4$. We find that the lowest-energy state for the Jain state shift ($\mathcal{S} = 4$) in larger system sizes has a total angular momentum $L^{\mathrm{tot}} \neq 0$, indicating that it represents excitations of some other incompressible state other than the Coulomb GS at $\nu = 12/5$ [27]. Second, the GSs with the $RR_3$ and BS shifts continue to have $L^{\mathrm{tot}} = 0$ for the systems that we have studied, and the extrapolation based on the result for $10 \leq N_e \leq 22$ leads to $E_0/N_e = -0.3425$ for the $RR_3$ state and $E_0/N_e = -0.3410$ for the BS state, respectively. Compared to the previous studies [25,31], the extrapolation errors are reduced by the inclusion of larger system sizes obtained using DMRG. Our calculations suggest that the GS state with shift $\mathcal{S} = -2(\mathcal{S} = 3)$ is energetically favored at $\nu = 12/5(13/5)$. Our results are consistent with the interpretation that the $RR_3$ state describes the true GS (see the full evidence below), while the other states at nearby shifts correspond to states with quasiparticle or quasihole excitations.

*Orbital ES.*—Li and Haldane first established that the orbital ES of the GS of the FQH phase contains information about the counting of their edge modes [34,37]. Thus, the orbital ES provides a "fingerprint" of the topological order, which can be used to identify the emergent topological phase in a microscopic Hamiltonian [34,39–42].

As a model FQH state, the $RR_3$ parafermion state can be represented by its highest-density root configuration pattern of 1110011100…11100111, corresponding to a generalized Pauli principle of no more than three electrons in five consecutive orbitals [67–69]. Consequently, the orbital ES depends on the number of electrons in the partitioned subsystem [49]. In Fig. 3, we show the orbital ES of three distinct partitions for system size $N_e = 36$ for the Coulomb GS. For $3n$ electrons in the subsystem [Fig. 3(a)], the leading ES displays the multiplicity pattern 1,1,3,6,12 in the first five angular momentum sectors $\Delta L_z^A = 0, 1, 2, 3, 4$. For $3n+1$ or $3n+2$ electrons in the subsystem [Figs. 3(b) and 3(c)], the ES shows the multiplicity pattern of 1,2,5,9 in the $\Delta L = 0, 1, 2, 3$ momentum sectors. The above characteristic multiplicity patterns of the low-lying ES agree with the predicted edge excitation spectrum of the $RR_3$ state obtained either from its associated CFT, or the "$\leq 3$ in 5" exclusion statistics rule [49].

In addition, we vary the Haldane pseudopotentials $\mathcal{V}^1(1)$ and $\mathcal{V}^1(3)$ (keeping all others at their Coulomb-interaction values), and we map out an ES-gap diagram which illustrates the robustness of the FQH state as the interaction parameters are changed [70–73]. In Fig. 3, we plot the entanglement gap (for the lowest-$L^z$ ES level) [34,46] as a function of $\mathcal{V}^1(1)/\mathcal{V}^1_{\mathrm{Coul}}(1)$ and $\mathcal{V}^1(3)/\mathcal{V}^1_{\mathrm{Coul}}(3)$, where $\mathcal{V}^1_{\mathrm{Coul}}(l)$ are the Coulomb values of pseudopotentials. We find that the entanglement gap is robust in a region centered

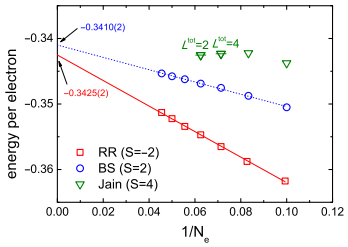


FIG. 2 (color online). Finite-size extrapolation of the GS energies for different shifts corresponding to different candidate states at $\nu = 12/5$. All energies have been rescaled by the renormalized magnetic length. The angular momentum of the GS is shown whenever it is nonzero ($L^{\mathrm{tot}} \neq 0$).

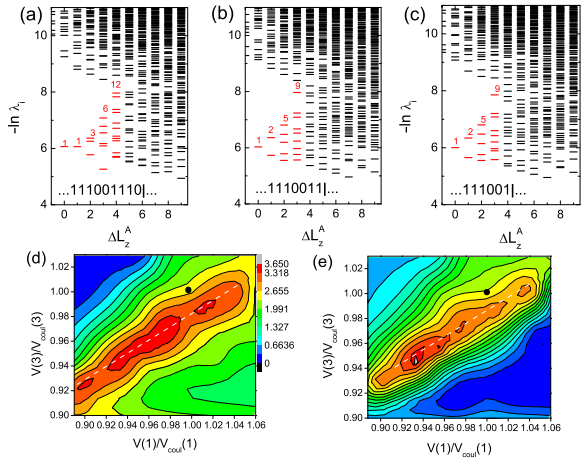


FIG. 3 (color online). (a)–(c) The low-lying orbital ES of $N_e = 36$ are shown for three different partitions. The lower ES level counting in the sector $\Delta L_z^A = 0, 1, 2, 3, 4$ are labeled by color, where $\Delta L_z^A = L_z^A - L_{z,\mathrm{min}}^A$, with $L_{z,\mathrm{min}}^A$ as the quantum number where the primary field occurs. The entanglement gap of orbital ES of $N_e = 24$ is shown for partition (d) with $3n$ electrons and (e) with $3n+1$ electrons in the subsystem as a function of the pseudopotentials $\mathcal{V}^1(1)/\mathcal{V}^1_{\mathrm{Coul}}(1)$ and $\mathcal{V}^1(3)/\mathcal{V}^1_{\mathrm{Coul}}(3)$, where $\mathcal{V}^1_{\mathrm{Coul}}(l)$ is the Coulomb value of the pseudopotentials. The black point corresponds to the Coulomb point.

at an approximately-fixed $\mathcal{V}^1(1)/\mathcal{V}^1(3)$ ratio (indicated by the white line). Away from that, for the regime $\mathcal{V}^1(1)/\mathcal{V}^1_{\mathrm{Coul}}(1) < 0.92$ and $\mathcal{V}^1(3)/\mathcal{V}^1_{\mathrm{Coul}}(3) > 0.98$, we find a rapid drop of the entanglement gap indicating a quantum phase transition. We have also studied the effect of the ES of modifying the Coulomb interaction with a realistic layer width $b$ [49], and we find that the $\mathrm{RR}_3$ state persists until $b/l_B \sim 2$, which is qualitatively consistent with the results of varying $\mathcal{V}^1(1)$ and $\mathcal{V}^1(3)$.

*Topological entanglement entropy.*—For a two-dimensional gapped topologically ordered state, the dependence of the entanglement entropy $S_A(l_A)$ of the subsystem A on the finite boundary-cut length $l_A$ has the form $S_A(l_A) = \alpha l_A - \gamma$, where TEE $\gamma$ is related to the total quantum dimension $\mathcal{D}$ by $\gamma = \ln \mathcal{D}$ [32,33]. We have extracted the TEE using our largest system, $N_e = 36$ [49]. The TEE obtained was $\gamma = 1.491 \pm 0.091$, consistent with the theoretically predicted value $\gamma = \ln \mathcal{D} = \ln \sqrt{5(1+\phi^2)} \approx 1.447$ for the $\mathrm{RR}_3$ state, where each non-Abelian Fibonacci anyon quasiparticle contributes an individual quantum dimension $d_F = \phi = (\sqrt{5}+1)/2$ ($\phi$ denotes the golden ratio). The appearance of $d_F = \phi$ is a signal of the emergence of Fibonacci anyon quasiparticles, and it arises because two Fibonacci quasiparticles may fuse either into the identity or into a single Fibonacci quasiparticle [45]. This exotic property makes Fibonacci quasiparticles capable of universal quantum computation [17].

*Topological degeneracy on the infinite cylinder.*—Topologically ordered states have characteristic GS degeneracies on compactified spaces. To access the different topological sectors at $\nu = 13/5$, we implemented the infinite-size DMRG in cylinder geometry with a finite circumference $L_y$ [42,49,74]. For each value of $L_y$, we repeatedly calculated GSs using different random initializations for the infinite DMRG optimization. We found that each infinite DMRG simulation converged to one of the two states: $|\Psi_1\rangle$ and $|\Psi_\phi\rangle$. These states are distinguishable by their orbital ES, as shown in Fig. 4: $|\Psi_1\rangle$ has the same ES structure as in Figs. 3(a)–3(c), which matches the identity sector with root configuration …0111001110…. On the other hand, $|\Psi_\phi\rangle$ shows the ES multiplicity pattern $1, 3, 6, 13, \ldots$, which identifies the spectrum as that of the Fibonacci non-Abelian sector with root configuration …1010110101… [49,75]. Furthermore, these two ground states are indeed energetically degenerate, with an energy difference per electron of less than 0.0002 with $L_y = 24 l_B$, while the entropy difference between these two states is around $\Delta S \approx \ln \phi \approx 0.48$, consistent with the quantum dimension of the Fibonacci quasiparticle. Combining this with the fivefold center-of-mass degeneracy, we have obtained all ten of the predicted degenerate $\mathrm{RR}_3$ GSs on infinite cylinder (or torus).

*Summary and discussion.*—We have presented what we believe to be compelling evidence that the essence of the Coulomb-interaction ground states at $\nu = 13/5$ and $12/5$ is indeed captured by the parafermion $k = 3$ Read-Rezayi state $\mathrm{RR}_3$, in which quasiparticles obey non-Abelian "Fibonacci anyon" statistics. The neutral-excitation gap is found to be a finite value $\Delta_n \approx 0.012 e^2/l_B$ in the thermodynamic limit. Results for the entanglement spectrum fingerprint and the value of the topological entanglement entropy show that the edge structure and bulk quasiparticle statistics are consistent with the prediction bases on the $\mathrm{RR}_3$ state. Additionally, we find two topologically degenerate ground-state sectors on the infinite cylinder, respectively, corresponding to the identity and the Fibonacci anyonic quasiparticle, which fully confirms the $\mathrm{RR}_3$ state, without input of any features (such as shift) taken from the model wave function, that might have biased the calculation. The current work opens up a number of directions deserving further exploration. For example, while the FQH $\nu = 12/5$ state has been observed in experiments, there is no evidence of a FQH phase at $\nu = 13/5$ in the same systems [5,8]. So far, it is not clear whether this absence is due to a broken particle-hole symmetry from Landau-level mixing, or other asymmetry effects such as differences in the quantum wells [7]. Our numerical studies suggest that the outlook for the existence of such a state at 13/5 is promising, and some positive signs of this may have already been observed very recently [76]. Numerical studies may also further suggest how various other exotic FQH states in the second Landau level at different filling factors may be stabilized.

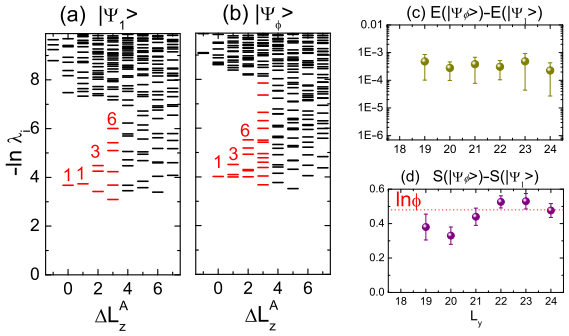


FIG. 4 (color online). (a),(b) The low-lying orbital ES of $\Psi_1$ and $|\Psi_\phi\rangle$ by setting $L_y = 24 l_B$. $|\Psi_{1(\phi)}\rangle$ denotes the GS with identity $\mathbb{1}$ (Fibonacci $\phi$) anyonic quasiparticle. (c) Energy difference and (d) entropy difference between $|\Psi_1\rangle$ and $|\Psi_\phi\rangle$, obtained from an infinite DMRG on cylinder geometry with varying $L_y$. The error bars are determined based on results from ten different infinite DMRG calculations for each sector [49].

W. Z. thanks Z. Liu for the fruitful discussion, N. Regnault and A. Wójs for their useful comments. We also thank X. G. Wen for the stimulating discussion and M. Zaletel, R. S. K. Mong, and F. Pollamann for the private communication prior to publication. This work is supported by the U.S. Department of Energy, Office of Basic Energy Sciences under Grants No. DE-FG02-06ER46305 (W. Z., D. N. S.) and No. DE-SC0002140 (F. D. M. H.), and the

National Science Foundation through Grant No. DMR-1408560 (S. S. G.). F. D. M. H. also acknowledges support from the W. M. Keck Foundation. W. Z. also acknowledges support from Grants No. MRSEC DMR-1420541 and No. PREM DMR-1205734 for a visit to Princeton, where this work was completed.

*Note added.*—Recently, we became aware of overlapping results in Ref. [77].

[1] D. C. Tsui, H. L. Stormer, and A. C. Gossard, Phys. Rev. Lett. **48**, 1559 (1982).
[2] R. B. Laughlin, Phys. Rev. Lett. **50**, 1395 (1983).
[3] R. Willett, J. P. Eisenstein, H. L. Stormer, D. C. Tsui, A. C. Gossard, and J. H. English, Phys. Rev. Lett. **59**, 1776 (1987).
[4] W. Pan, J.-S. Xia, V. Shvarts, D. E. Adams, H. L. Stormer, D. C. Tsui, L. N. Pfeiffer, K. W. Baldwin, and K. W. West, Phys. Rev. Lett. **83**, 3530 (1999).
[5] J. S. Xia, W. Pan, C. L. Vicente, E. D. Adams, N. S. Sullivan, H. L. Stormer, D. C. Tsui, L. N. Pfeiffer, K. W. Baldwin, and K. W. West, Phys. Rev. Lett. **93**, 176809 (2004).
[6] H. C. Choi, W. Kang, S. Das Sarma, L. N. Pfeiffer, and K. W. West, Phys. Rev. B **77**, 081301(R) (2008).
[7] W. Pan, J. S. Xia, H. L. Stormer, D. C. Tsui, C. Vicente, E. D. Adams, N. S. Sullivan, L. N. Pfeiffer, K. W. Baldwin, and K. W. West, Phys. Rev. B **77**, 075307 (2008).
[8] A. Kumar, G. A. Csathy, M. J. Manfra, L. N. Pfeiffer, and K. W. West, Phys. Rev. Lett. **105**, 246808 (2010).
[9] I. P. Radu, J. B. Miller, C. M. Marcus, M. A. Kastner, L. N. Pfeiffer, and K. W. West, Science **320**, 899 (2008).
[10] M. Dolev, M. Heiblum, V. Umansky, A. Stern, and D. Mahalu, Nature (London) **452**, 829 (2008).
[11] R. L. Willett, C. Nayak, K. Shtengel, L. N. Pfeiffer, and K. W. West, Phys. Rev. Lett. **111**, 186401 (2013).
[12] S. Baer, C. Rossler, T. Ihn, K. Ensslin, C. Reichl, and W. Wegscheider, Phys. Rev. B **90**, 075403 (2014).
[13] C. Zhang, C. Huan, J. S. Xia, N. S. Sullivan, W. Pan, K. W. Baldwin, K. W. West, L. N. Pfeiffer, and D. C. Tsui, Phys. Rev. B **85**, 241302(R) (2012).
[14] G. Moore and N. Read, Nucl. Phys. **B360**, 362 (1991).
[15] M. Greiter, X. G. Wen, and F. Wilczek, Phys. Rev. Lett. **66**, 3205 (1991).
[16] N. Read and E. Rezayi, Phys. Rev. B **59**, 8084 (1999).
[17] C. Nayak, S. H. Simon, A. Stern, M. Freedman, and S. D. Sarma, Rev. Mod. Phys. **80**, 1083 (2008).
[18] A. Y. Kitaev, Ann. Phys. (Amsterdam) **303**, 2 (2003).
[19] M. H. Freedman, M. Larsen, and Z. Wang, Commun. Math. Phys. **227**, 605 (2002).
[20] S. Das Sarma, M. Freedman, and C. Nayak, Phys. Rev. Lett. **94**, 166802 (2005).
[21] L. Hormozi, G. Zikos, N. E. Bonesteel, and S. H. Simon, Phys. Rev. B **75**, 165310 (2007).
[22] N. E. Bonesteel, L. Hormozi, G. Zikos, and S. H. Simon, Phys. Rev. Lett. **95**, 140503 (2005).
[23] E. H. Rezayi and N. Read, Phys. Rev. B **79**, 075306 (2009).
[24] P. Bonderson and J. K. Slingerland, Phys. Rev. B **78**, 125323 (2008).
[25] P. Bonderson, A. E. Feiguin, G. Moller, and J. K. Slingerland, Phys. Rev. Lett. **108**, 036806 (2012).
[26] G. J. Sreejith, C. Toke, A. Wojs, and J. K. Jain, Phys. Rev. Lett. **107**, 086806 (2011).
[27] G. J. Sreejith, Y.-H. Wu, A. Wojs, and J. K. Jain, Phys. Rev. B **87**, 245125 (2013).
[28] F. D. M. Haldane, Phys. Rev. Lett. **51**, 605 (1983).
[29] B. I. Halperin, Phys. Rev. Lett. **52**, 1583 (1984).
[30] J. K. Jain, *Composite Fermions* (Cambridge University Press, Cambridge, England, 2007).
[31] A. Wojs, Phys. Rev. B **80**, 041104(R) (2009).
[32] A. Kitaev and J. Preskill, Phys. Rev. Lett. **96**, 110404 (2006).
[33] M. Levin and X.-G. Wen, Phys. Rev. Lett. **96**, 110405 (2006).
[34] H. Li and F. D. M. Haldane, Phys. Rev. Lett. **101**, 010504 (2008).
[35] Y. Zhang, T. Grover, A. Turner, M. Oshikawa, and A. Vishwanath, Phys. Rev. B **85**, 235151 (2012).
[36] X. G. Wen, Int. J. Mod. Phys. B **04**, 239 (1990).
[37] X. G. Wen, Adv. Phys. **44**, 405 (1995).
[38] M. Haque, O. Zozulya, and K. Schoutens, Phys. Rev. Lett. **98**, 060401 (2007).
[39] A. M. Lauchli, E. J. Bergholtz, J. Suorsa, and M. Haque, Phys. Rev. Lett. **104**, 156404 (2010).
[40] Z. Papic, B. A. Bernevig, and N. Regnault, Phys. Rev. Lett. **106**, 056801 (2011).
[41] L. Cincio and G. Vidal, Phys. Rev. Lett. **110**, 067208 (2013).
[42] M. P. Zaletel, R. S. K. Mong, and F. Pollmann, Phys. Rev. Lett. **110**, 236801 (2013).
[43] H. H. Tu, Y. Zhang, and X. L. Qi, Phys. Rev. B **88**, 195412 (2013).
[44] H. C. Jiang, Z. H. Wang, and L. Balents, Nat. Phys. **8**, 902 (2012).
[45] W. Zhu, S. S. Gong, F. D. M. Haldane, and D. N. Sheng, Phys. Rev. Lett. **112**, 096803 (2014).
[46] J. Z. Zhao, D. N. Sheng, and F. D. M. Haldane, Phys. Rev. B **83**, 195135 (2011).
[47] G. Fano, F. Ortolani, and E. Colombo, Phys. Rev. B **34**, 2670 (1986).
[48] M. Greiter, Phys. Rev. B **83**, 115129 (2011).
[49] See Supplemental Material at http://link.aps.org/supplemental/10.1103/PhysRevLett.115.126805, which includes Refs. [50–55], for details of Haldane pseudopotentials used for calculation, a detailed analysis of edge excitations of Read-Rezayi $k = 3$ state, the effect of finite layer-width on ES, the topological entanglement entropy, and the numerical details of the infinite-size DMRG algorithm on cylinder geometry.
[50] D. Yoshioka, J. Phys. Soc. Jpn. **55**, 885 (1986).
[51] T. T. Wu and C. N. Yang, Phys. Rev. D **77**, 1018 (1977).
[52] R. E. Wooten, Bull. Am. Phys. Soc. (2015).
[53] O. S. Zozulya, M. Haque, K. Schoutens, and E. H. Rezayi, Phys. Rev. B **76**, 125310 (2007).
[54] B. Estienne, N. Regnault, and B. A. Bernevig, Phys. Rev. Lett. **114**, 186801 (2015).
[55] I. P. McCulloch, arXiv:0804.2509.
[56] S. R. White, Phys. Rev. Lett. **69**, 2863 (1992).
[57] T. Xiang, Phys. Rev. B **53**, R10445(R) (1996).
[58] N. Shibata and D. Yoshioka, Phys. Rev. Lett. **86**, 5755 (2001).

[59] A. E. Feiguin, E. Rezayi, C. Nayak, and S. Das Sarma, Phys. Rev. Lett. **100**, 166803 (2008).
[60] Z. X. Hu, Z. Papic, S. Johri, R. N. Bhatt, and P. Schmitteckert, Phys. Lett. A **376**, 2157 (2012).
[61] R. Morf, N. d'Ambrumenil, and B. I. Halperin, Phys. Rev. B **34**, 3037 (1986).
[62] The charged gap is out of the scope of the current study.
[63] F. D. M. Haldane and E. H. Rezayi, Phys. Rev. Lett. **54**, 237 (1985).
[64] S. M. Girvin, A. H. MacDonald, and P. M. Platzman, Phys. Rev. Lett. **54**, 581 (1985).
[65] B. Yang, Z.-X. Hu, Z. Papic, and F. D. M. Haldane, Phys. Rev. Lett. **108**, 256807 (2012).
[66] While the obtained $\Delta_n \approx 0.012$ is close to the experimental estimated value ($\sim$0.016) at $\nu = 12/5$ [8], the asymmetry between $\nu = 12/5$ and $13/5$ in experiments may dependent on the details of the systems and the Landau-level coupling, which is beyond the scope of the current Letter and is left for future study.
[67] E. J. Bergholtz and A. Karlhede, Phys. Rev. Lett. **94**, 026802 (2005).
[68] B. A. Bernevig and F. D. M. Haldane, Phys. Rev. Lett. **100**, 246802 (2008).
[69] B. A. Bernevig and F. D. M. Haldane, Phys. Rev. B **77**, 184502 (2008).
[70] M. R. Peterson, T. Jolicoeur, and S. Das Sarma, Phys. Rev. B **78**, 155308(2008).
[71] M. Storni, R. H. Morf, and S. Das Sarma, Phys. Rev. Lett. **104**, 076803 (2010).
[72] J. Biddle, M. R. Peterson, and S. Das Sarma, Phys. Rev. B **84**, 125141 (2011).
[73] K. Pakrouski, M. R. Peterson, T. Jolicoeur, V. W. Scarola, C. Nayak, and M. Troyer, Phys. Rev. X **5**, 021004 (2015).
[74] M. P. Zaletel, R. S. K. Mong, F. Pollmann, and E. H. Rezayi, Phys. Rev. B **91**, 045115 (2015).
[75] The ES results shown in this Letter give an unambiguous confirmation of the $RR_3$ state as the ground state at $\nu = 12/5$ and $13/5$. Based on this measurement, we can also exclude the possibility of the Jain CF state, because the Jain state is expected to show a $1, 2, 5, \ldots$ degeneracy pattern in ES.
[76] J. Falson, D. Maryenko, B. Friess, D. Zhang, Y. Kozuka, A. Tsukazaki, J. H. Smet, and M. Kawasaki, Nat. Phys. **11**, 347 (2015).
[77] R. S. K. Mong, M. P. Zaletel, F. Pollmann, and Z. Papić, arXiv:1505.02843.